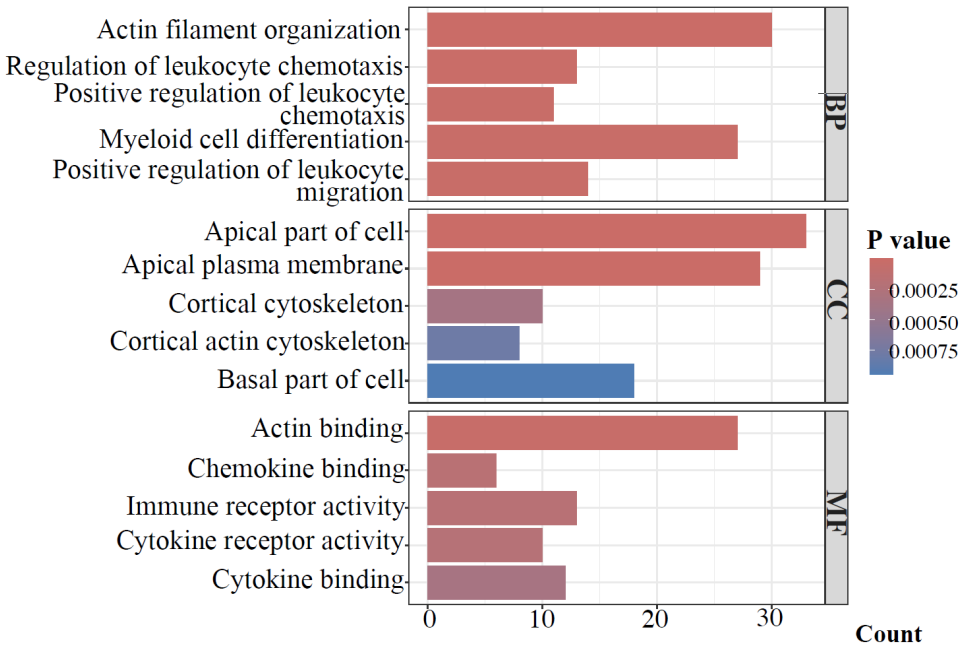


**Figure S1** Gene ontology (GO) enrichment in three main terms.


https://dx.doi.org/10.21037/jgo-2025-1-968

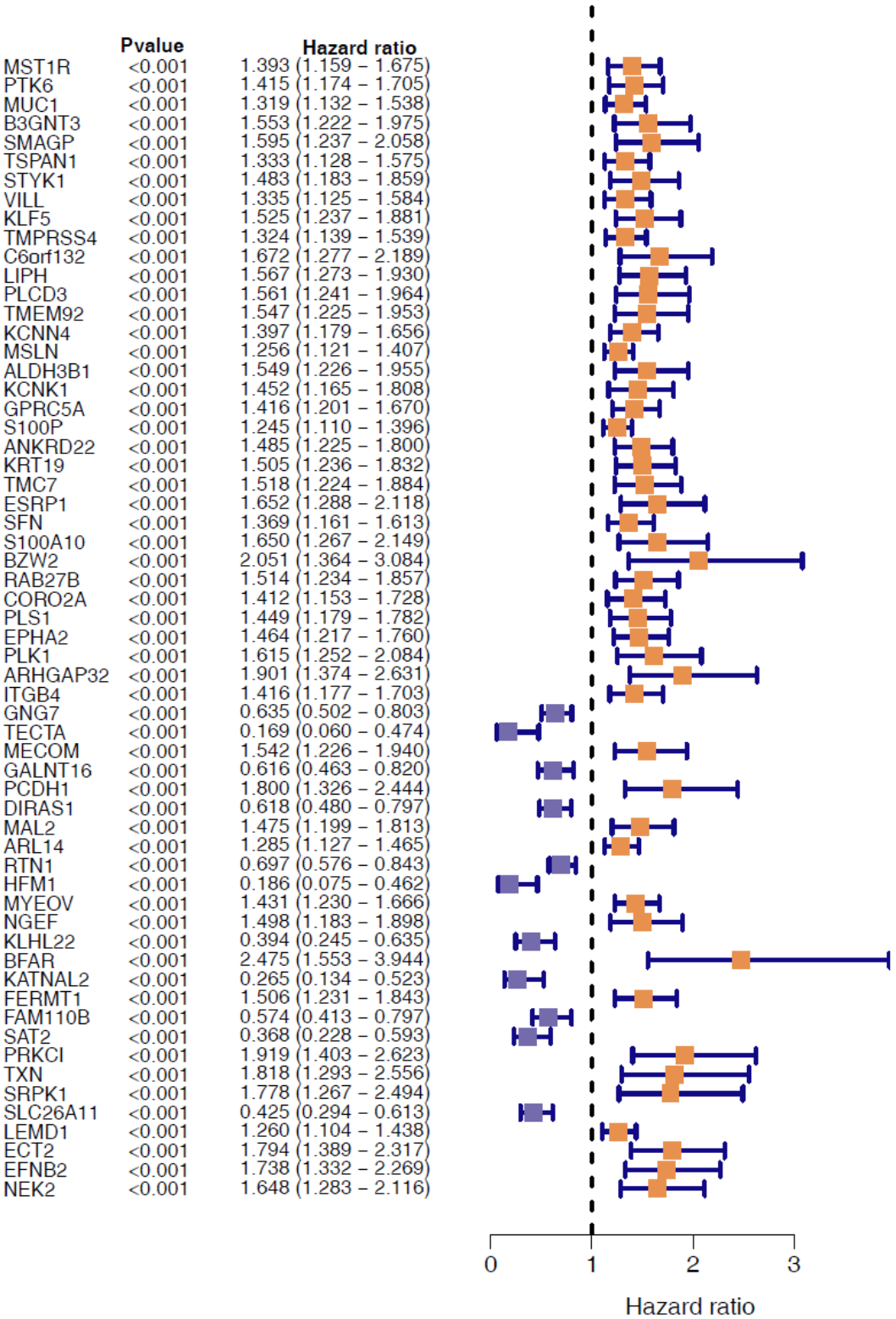


**Figure S2** The forest plot displayed that univariate Cox analysis for the screening of overall survival-associated TRPM4-related signature by TCGA-PAAD.


https://dx.doi.org/10.21037/jgo-2025-1-968

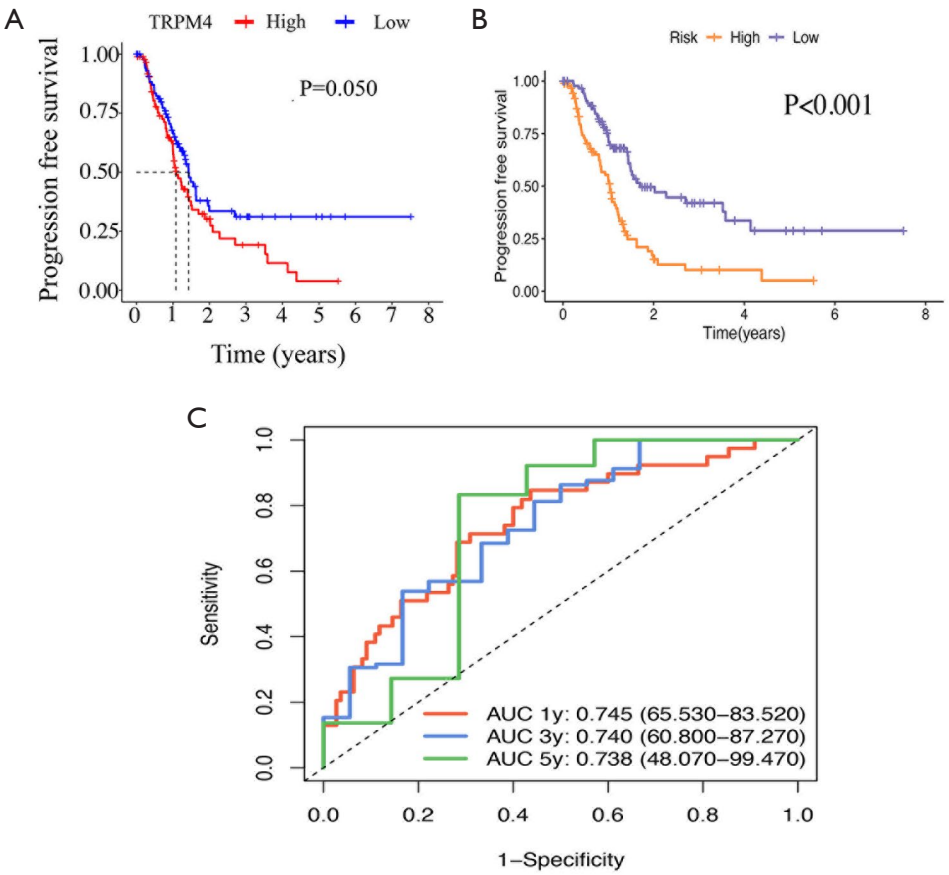


**Figure S3** TCGA-PAAD datasets verified the model. It provided the progression-free survival on TRPM4 (A) and risk score (B). ROC showed the specificity and sensitivity of our gene and its signature with survival rate on risk score (C). AUC, area under the curve; CI, confidence interval; ROC, receiver operating characteristic.


https://dx.doi.org/10.21037/jgo-2025-1-968

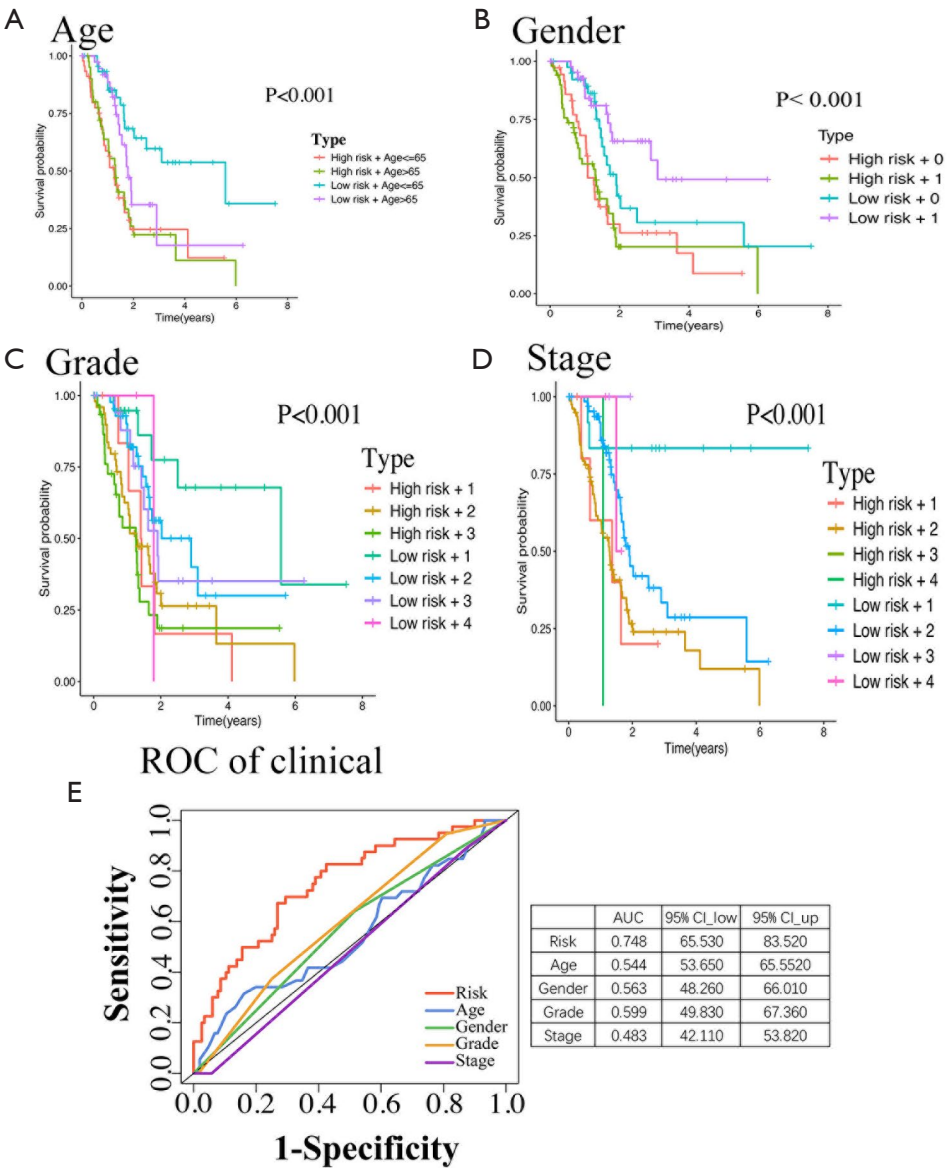


| | AUC | 95% CI_low | 95% CI_up |
|---|---|---|---|
| Risk | 0.748 | 65.530 | 83.520 |
| Age | 0.544 | 53.650 | 65.5520 |
| Gender | 0.563 | 48.260 | 66.010 |
| Grade | 0.599 | 49.830 | 67.360 |
| Stage | 0.483 | 42.110 | 53.820 |

**Figure S4** Association between clinicopathological characteristics and risk score. Overall survival between prognostic risk score and age (A), and gender (0 female, 1 male) (B), and grades (1, 2, 3 means grade 1, 2, 3) (C), and stages (1, 2, 3, 4 means stage I, II, III, IV) (D). Receiver operating characteristic value shows prognostic risk and clinicopathological traits (E). Grades indicate tumor grade levels (1–4). High-risk group includes grades 1–3, while low-risk group includes grades 1–4. AUC, area under the curve; CI, confidence interval; ROC, receiver operating characteristic.


https://dx.doi.org/10.21037/jgo-2025-1-968

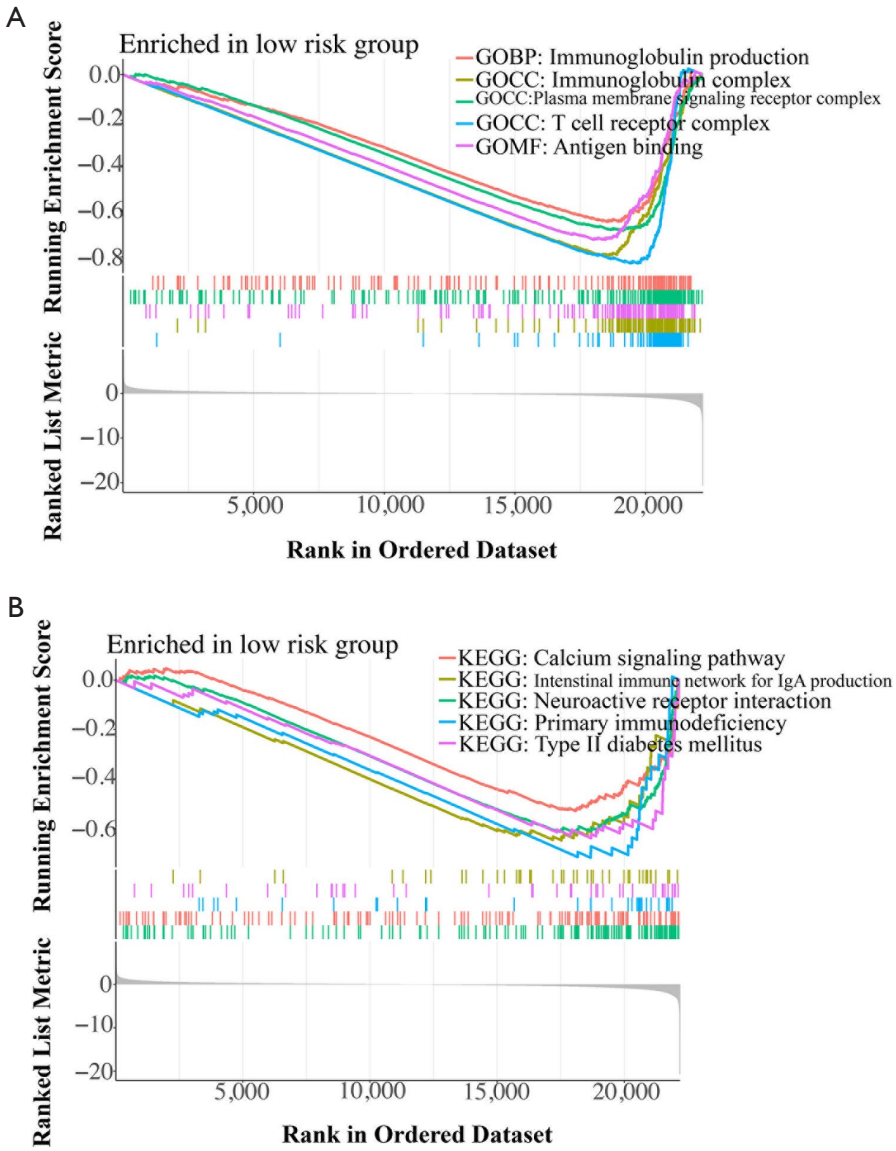


**Figure S5** GSEA for the low-risk group. The enrichment of GO-based GSEA (A) and KEGG-based GSEA (B).


https://dx.doi.org/10.21037/jgo-2025-1-968

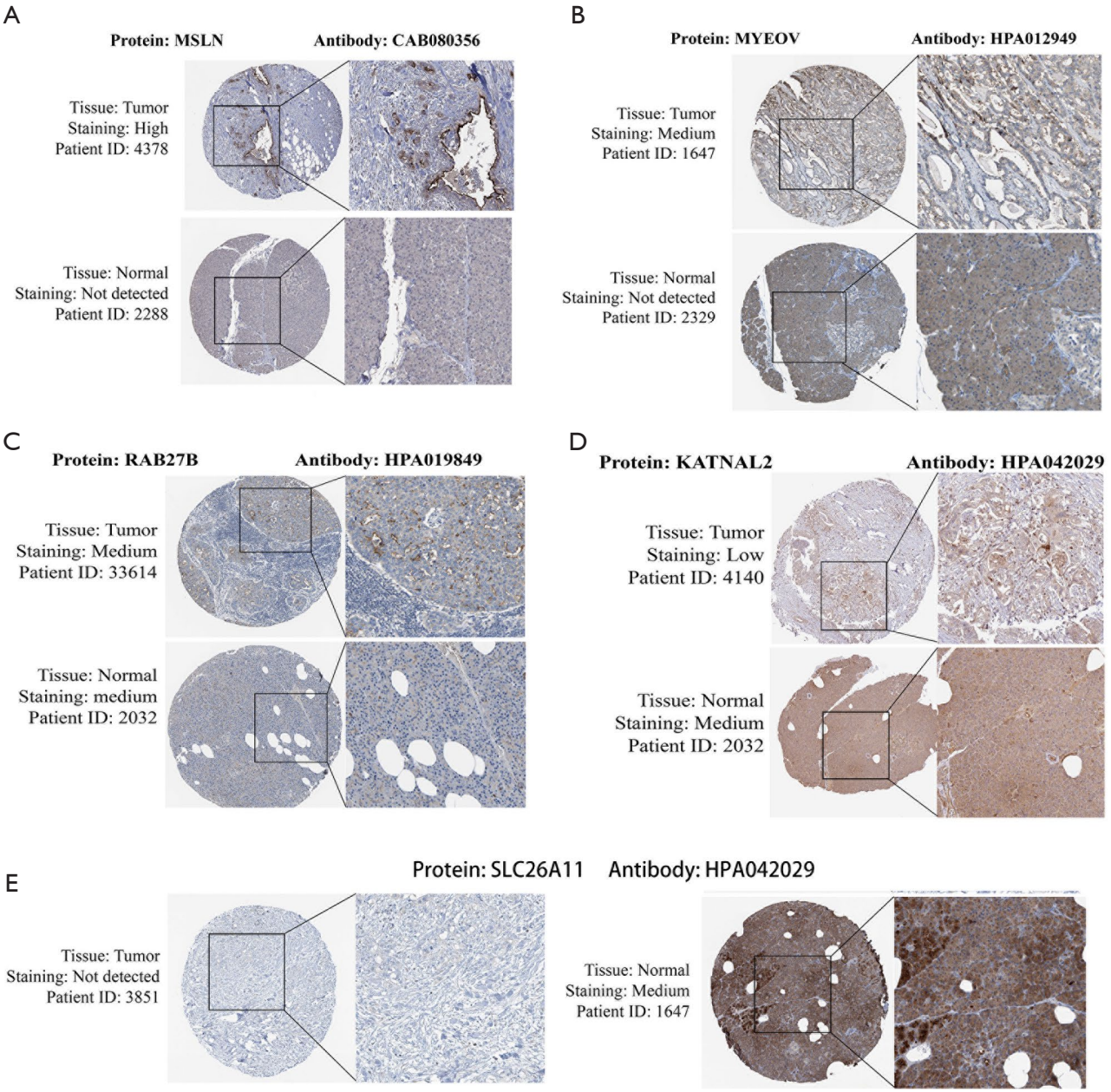


**Figure S6** Protein expression of genes included in the TRPM4-associated prognostic signature in pancreatic tissues. For each gene, immunohistochemical (IHC) images of normal pancreatic tissue and pancreatic cancer tissue are shown (as provided by the Human Protein Atlas, HPA). Genes displayed include MSLN (A), MYEOV (B), RAB27B (C), KATNAL2 (D), and SLC26A11 (E). HPA URLs: MSLN, [https://www.proteinatlas.org/ENSG00000102854-MSLN/tissue/pancreas, https://www.proteinatlas.org/ENSG00000102854-MSLN/cancer/pancreatic+cancer#PAAD_validation]; MYEOV, [https://www.proteinatlas.org/ENSG00000172927-MYEOV/tissue/pancreas, https://www.proteinatlas.org/ENSG00000172927-MYEOV/cancer/pancreatic+cancer#PAAD_validation]; RAB27B, [https://www.proteinatlas.org/ENSG00000041353-RAB27B/tissue/pancreas, https://www.proteinatlas.org/ENSG00000041353-RAB27B/cancer/pancreatic+cancer#PAAD_validation]; KATNAL2, [https://www.proteinatlas.org/ENSG00000167216-KATNAL2/tissue/pancreas, https://www.proteinatlas.org/ENSG00000167216-KATNAL2/cancer/pancreatic+cancer#PAAD_validation]; SLC26A11, [https://www.proteinatlas.org/ENSG00000181045-SLC26A11/tissue/pancreas, https://www.proteinatlas.org/ENSG00000181045-SLC26A11/cancer/pancreatic+cancer#PAAD_TCGA]. HPA, Human Protein Atlas; IHC, immunohistochemistry.


https://dx.doi.org/10.21037/jgo-2025-1-968

**Table S1** Drug sensitivity screening results based on TCGA and GEO datasets

| TCGA drug | Gene expression with high IC50 | GEO drug | Gene expression with high IC50 |
|---|---|---|---|
| Afuresertib | High | Afuresertib | High |
| AGI-5198 | High | AGI-5198 | High |
| AGI-6780 | High | AGI-6780 | High |
| Alisertib | High | Alisertib | High |
| AMG-319 | High | AMG-319 | High |
| AT13148 | High | AT13148 | High |
| Axitinib | High | Axitinib | High |
| AZD1208 | High | AZD1208 | High |
| AZD2014 | High | AZD2014 | High |
| AZD4547 | High | AZD4547 | High |
| AZD5153 | High | AZD5153 | High |
| AZD5363 | High | AZD5363 | High |
| AZD5991 | High | AZD5991 | High |
| AZD8055 | High | AZD8055 | High |
| BIBR-1532 | High | BIBR-1532 | High |
| BMS-754807 | High | BMS-754807 | High |
| CDK9_5038 | High | CDK9_5038 | High |
| Cyclophosphamide | High | Cyclophosphamide | High |
| CZC24832 | High | CZC24832 | High |
| Dabrafenib | High | Dabrafenib | High |
| Dihydrorotenone | High | Dihydrorotenone | High |
| Doramapimod | High | Doramapimod | High |
| Eg5_9814 | Low | Eg5_9814 | High |
| Elephantin | High | Elephantin | High |
| Entinostat | High | Entinostat | High |
| EPZ004777 | High | EPZ004777 | High |
| EPZ5676 | High | EPZ5676 | High |
| Foretinib | High | Foretinib | High |
| Fulvestrant | High | Fulvestrant | High |
| Gallibiscoquinazole | High | Gallibiscoquinazole | High |
| GSK343 | High | GSK343 | High |
| GSK269962A | High | GSK269962A | High |
| GSK1904529A | High | GSK1904529A | High |
| GSK2578215A | High | GSK2578215A | High |
| GSK2606414 | High | GSK2606414 | High |

**Table S1** *(continued)*


https://dx.doi.org/10.21037/jgo-2025-1-968

**Table S1** *(continued)*

| TCGA drug | Gene expression with high IC50 | GEO drug | Gene expression with high IC50 |
|---|---|---|---|
| I-BET-762 | High | I-BET-762 | High |
| I-BRD9 | High | I-BRD9 | High |
| IAP_5620 | High | IAP_5620 | High |
| Ipatasertib | High | Ipatasertib | High |
| IRAK4_4710 | High | IRAK4_4710 | High |
| Irinotecan | High | Irinotecan | High |
| IWP-2 | High | IWP-2 | High |
| JAK1_8709 | High | JAK1_8709 | High |
| JQ1 | High | JQ1 | High |
| KRAS (G12C) Inhibitor-12 | High | KRAS (G12C) Inhibitor-12 | High |
| LCL161 | High | LCL161 | High |
| Leflunomide | High | Leflunomide | High |
| LGK974 | High | LGK974 | High |
| Linsitinib | High | Linsitinib | High |
| LJI308 | High | LJI308 | High |
| LY2109761 | High | LY2109761 | High |
| MIRA-1 | High | MIRA-1 | High |
| Mirin | High | Mirin | High |
| Mitoxantrone | High | Mitoxantrone | High |
| MK-2206 | High | MK-2206 | High |
| ML323 | High | ML323 | High |
| Nilotinib | High | Nilotinib | High |
| Niraparib | High | Niraparib | High |
| Nutlin-3a (-) | High | Nutlin-3a (-) | High |
| NVP-ADW742 | High | NVP-ADW742 | High |
| Obatoclax Mesylate | High | Obatoclax Mesylate | High |
| OF-1 | High | OF-1 | High |
| Olaparib | High | Olaparib | High |
| Oxaliplatin | High | Oxaliplatin | High |
| P22077 | High | P22077 | High |
| PAK_5339 | High | PAK_5339 | High |
| Palbociclib | High | Palbociclib | High |
| PCI-34051 | High | PCI-34051 | High |
| PFI3 | High | PFI3 | High |

**Table S1** *(continued)*


https://dx.doi.org/10.21037/jgo-2025-1-968

**Table S1** *(continued)*

| TCGA drug | Gene expression with high IC50 | GEO drug | Gene expression with high IC50 |
|---|---|---|---|
| Picolinici-acid | High | Picolinici-acid | High |
| Podophyllotoxin bromide | High | Podophyllotoxin bromide | High |
| PRIMA-1MET | High | PRIMA-1MET | High |
| Rapamycin | High | Rapamycin | High |
| Ribociclib | High | Ribociclib | High |
| RO-3306 | High | RO-3306 | High |
| RVX-208 | High | RVX-208 | High |
| Sabutoclax | High | Sabutoclax | High |
| SB216763 | High | SB216763 | High |
| SCH772984 | Low | SCH772984 | Low |
| Selumetinib | Low | Selumetinib | Low |
| Sorafenib | High | Sorafenib | Low |
| TAF1_5496 | High | TAF1_5496 | High |
| Tamoxifen | High | Tamoxifen | High |
| Telomerase Inhibitor IX | High | Telomerase Inhibitor IX | High |
| Teniposide | High | Teniposide | High |
| Topotecan | High | Topotecan | High |
| Tozasertib | High | Tozasertib | High |
| Trametinib | Low | Trametinib | Low |
| Uprosertib | High | Uprosertib | High |
| Venetoclax | High | Venetoclax | High |
| Vincristine | High | Vincristine | High |
| Vorinostat | High | Vorinostat | High |
| Wnt-C59 | High | Wnt-C59 | High |
| Zoledronate | High | Zoledronate | High |

Drug sensitivity was inferred based on the association between gene expression levels and predicted half-maximal inhibitory concentration (IC50) values derived from TCGA and GEO datasets. “High” and “low” indicate relatively higher or lower predicted IC50 values, respectively, suggesting reduced or increased drug sensitivity. These results are based on computational prediction and are intended for exploratory analysis.


https://dx.doi.org/10.21037/jgo-2025-1-968